

MEASUREMENT OF GAS DISCHARGE COEFFICIENT

Iлона Pasková, Ondřej Novák, Václav Koza

RWE GasNet, ilona.paskova@rwe.cz

ICT Prague, Department of gas, coke and air protection, ondrej.novak@vscht.cz, vaclav.koza@vscht.cz

In case of gas pipeline leakage the gas leakage volume must be determined to calculate costs and losses of the accident. In order to calculate the exact volume of leaked gas it is necessary to specify the cross-section and discharge coefficient of the leak. The laboratory apparatus for the discharge coefficient determination has been built. The vessel pressurized by the gas is freely emptied through the studied orifice into the space at atmospheric pressure. Time course of the pressure and temperature of gas in the vessel is measured and evaluated in the form of the discharge coefficient. Data on several types of orifice (circular, triangular, square shaped, long narrow slot, flapped semi-open cut in the metal sheet) were measured in critical and sub-critical flow regime.

Key words: discharge coefficient, compressible flow, unsteady flow, discharge from a vessel

Received 27. 5. 2013, accepted 26. 6. 2013

1. Introduction

In order to assess the leakage from gas pipelines it is problematic to find exact properties of the orifice which the gas leaked through. These properties may be represented by the orifice cross-section area and the value of the orifice discharge coefficient. The discharge coefficient is treated as a parameter of an orifice that affects the area of the orifice for further computation [1]. Discharge coefficient values have been published for regular orifice shapes (aperture, jet) only and they are missing for irregular orifice shapes, which are in particular any cracks in the pipe wall.

It is impossible to treat all the factors that might influence practical discharge process. Even for relatively simple case of steady flow through an orifice several mathematical and semi-empirical solutions were obtained for well-defined sharp-edged orifices [2][3].

Discharge process is influenced by shape and width of the orifice and even by quality and shape of the upstream edge of it [4][5].

Thermodynamic parameters of the gas inside vessel are changing during the discharge process[6].

Temperature of the gas in the vessel during the discharge from the vessel is bounded on the one side by temperature computed from adiabatic expansion and on the other side by the constant temperature of the gas at the beginning of the discharge process [7].

In this paper we propose measurements of discharge coefficient for several types of orifices with different shapes and other properties.

The built detection device makes possible to determine the values of discharge coefficient for given particular orifice by measuring of the pressure decrease during the emptying of pressurized vessel to the atmosphere through the measured orifice.

The mass flow of a gas is characterized by this common equation:

$$\dot{m} = S\alpha\rho v, \quad (1)$$

where

- \dot{m} mass flow rate [kg s⁻¹]
- ρ density of the gas [kg m⁻³]
- α discharge coefficient [-]
- S orifice cross-section flow area [m²]
- v gas velocity [m s⁻¹].

From this equation follows that mass flow rate depends directly and proportionately on the discharge coefficient [8].

2. An experimental device

An experimental device schematically shown in the Fig. 1 is composed of these parts: Gas is supplied from the high pressure gas cylinders (1). They are standard gas cylinders with total volume of 50 l and working overpressure of 20 MPa. The cylinders are fitted with pressure reducers and connected to supply pipes with shutting valves (2) and (3). The connection of the valves is 1/2". Main inlet is controlled by a ball valve (4) with 1/2" connection. Safe working overpressure inside the apparatus is provided by relief valve (5), which is configured for maximum overpressure of 1 MPa. A welded vertical steel pressure vessel is used as the main pressure vessel of the experimental device (6). The pressure vessel is a standard expansion pressure vessel Aquamat P produced by Dukla Trutnov company. The entire vessel is zinc coated (inside and outside) and designed for working overpressure 1 MPa in maximum. Volume of the vessel is 163.15 l. Vessel Aquamat P has four connection points G1"- input, output and two

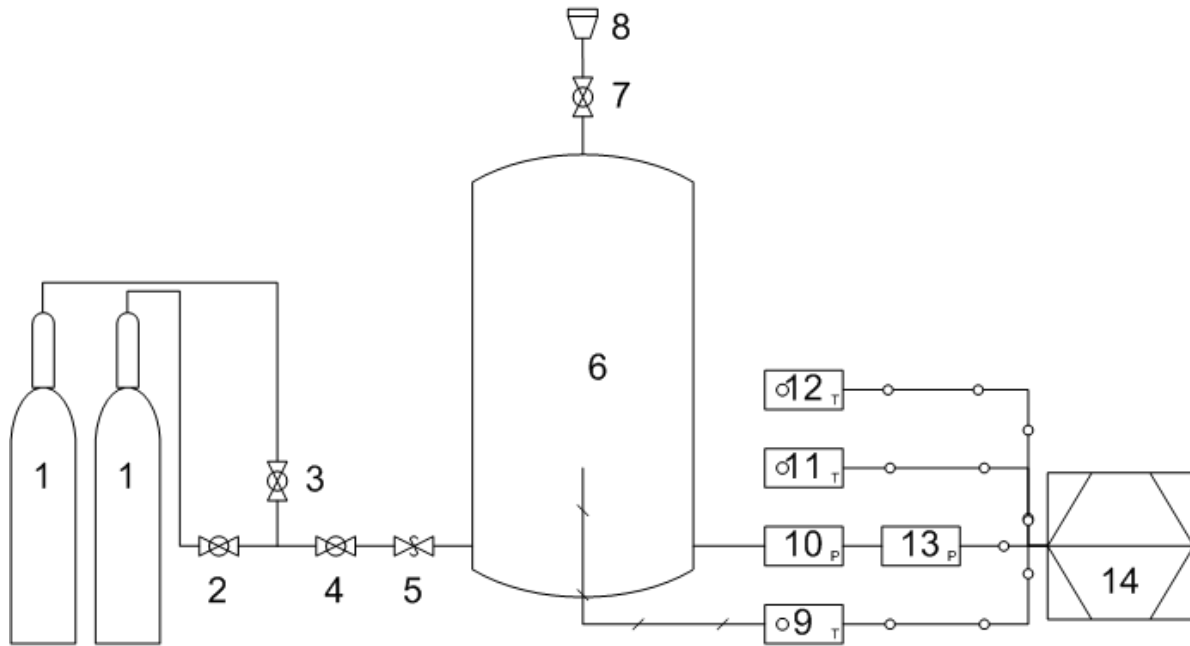


Fig. 1 block diagram of the experimental device. 1 supply gas tanks, 2 shutting valve, 3 shutting valve, 4 ball valve, 5 relief valve, 6 pressure vessel, 7 ball valve, 8 flange, 9 thermocouple, 10 pressure gauge with visible scale, 11 thermocouple, 12 sensor Pt100, 13 electronic pressure sensor, 14 computer



Fig. 2 picture of the measurement vessel



Fig. 3 detail of the flange with a measured orifice

connectors for the pressure and temperature sensors. A ball valve (7) is connected to the vessel by 1/2'' connection and controls flow through flange (8). The flange is a polyethylene flange G1'' secured by four screws - see the Fig. 3. Samples are inserted between two parts of the flange. The samples are steel sheets with orifices simulating the real disruption (controlled irregular orifice shapes) of a gas pipeline. Following figures show several samples – Fig. 4, 5, 6, 7. Temperature inside the

vessel is measured by a T type thermocouple Omega (9) with 1/16'' diameter and 12'' length. Pressure inside the vessel is measured by a gauge with visible scale (10) and an industrial pressure sensor DMP 331 (13). The sensor is converting gas pressure into an electrical current signal 4-20 mA. Ambient temperature is measured by a T type Omega thermocouple (11) with 1/16'' diameter and 12'' length. A temperature sensor Pt 100 (12) is used for measuring ambient temperature and to

supply reference temperature for thermocouples. The temperature sensor measurement range is $-40\text{ }^{\circ}\text{C}$ to $100\text{ }^{\circ}\text{C}$. The temperature sensor is connected to the power converter PTC/I, which converts changes in resistance of the sensor Pt 100 to the current signal 4-20 mA. All sensors are connected to an A/D converter and computer (14).

For the calculation of discharge coefficient two basic types of orifices were used:

- 1 Regular orifices with circular opening
- 2 Irregular orifices

Ad 1 Regular orifice in circle shape

Orifice samples were created from brass. Two series of circular orifices were created with different thickness in orifice point and diameters from 2 mm to about 18 mm.

Examples of orifices with regular opening shape:



Fig. 4 Example of the orifice with regular opening shape, screen diameter is 2.17 mm.



Fig. 5 Example of the orifice with regular opening shape, screen diameter is 18.29 mm.

Ad 2 Irregular orifices

Irregular opening samples were created from stainless sheet in thickness 2 mm. The measured opening is located in the center of plate; holes for flange's screws are located in corners. Examples of orifices with a real irregular opening shape with 3D character:

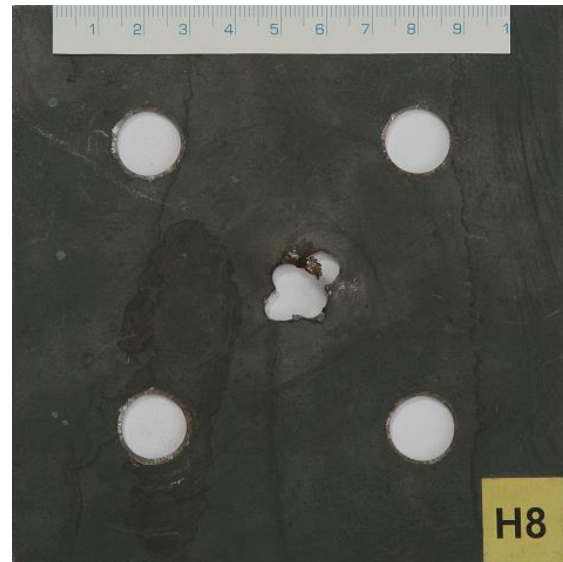


Fig. 6 Example of the orifice with irregular opening shape

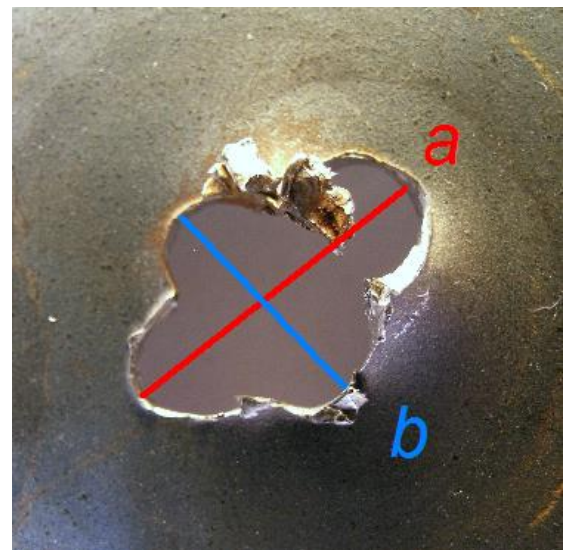


Fig. 7 Example of the orifice with irregular opening shape in detail, $a=19.2\text{ mm}$, $b=13.5\text{ mm}$

Finally, 3D orifices simulating the pipeline damage caused by building machinery were made for testing. Model of such orifice is in Fig. 8. This type of orifices we called as *lifted*. Orifice of this type consists of a 2D opening and a three-dimensional lifted flap, which may change effective area of the orifice and consequently the discharge coefficient (Fig. 9). Area of the lifted part of orifice, which is used for calculation, is the free flow area of the 2D part of the orifice.

Table 1 Parameters of tested orifices

Label	Shape	S [mm ²]	Thickness [mm]	Angle of lift [°]
1.1	Circular	3.27	0.6	-
1.2	Circular	7.79	0.6	-
1.3	Circular	15.34	0.6	-
1.4	Circular	28.27	0.6	-
1.5	Circular	62.77	0.6	-
1.6	Circular	110.47	0.6	-
1.7	Circular	260.16	0.6	-
2.1	Circular	3.70	10.0	-
2.2	Circular	7.40	10.0	-
2.3	Circular	15.00	10.0	-
2.4	Circular	26.79	10.0	-
2.5	Circular	64.33	10.0	-
2.6	Circular	111.59	10.0	-
2.7	Circular	262.73	10.0	-
S1	Narrow rectangular slot	5.16	1.6	-
S2	Narrow rectangular slot	18.95	1.6	-
C1.1	Square	28.62	1.6	-
C2.1	Square	113.42	1.6	-
C2.1	Square	93.72	1.6	33
C2.3	Square	84.14	1.6	52
T1.1	Triangular	22.45	1.6	-
T2.1	Triangular	99.39	1.6	-
T2.2	Triangular	90.90	1.6	33
T2.3	Triangular	94.69	1.6	43

Measurement procedure:

The measured orifice sample is inserted and fastened into the flange 8 and valve 7 is closed. Pressure vessel 6 is pressurized with gas from supply tanks up to maximum overpressure 1 MPa. Ball cock 4 is closed and this secures stop of filling the vessel. Pressure inside the vessel is recorded into PC by digital pressure sensor as well as actual temperatures inside and outside the vessel by two thermocouples and Pt100 sensor. Sampling frequency of reading the sensors is 100 Hz. After pressurization of the vessel to appropriate pressure inside the ball valve 7 is opened and the discharge starts. The gas escapes from the vessel 6 through the measured orifice. Flushing time depends on the initial pressure in the vessel and the size and shape of the measured orifice, which is characterized by the discharge coefficient.

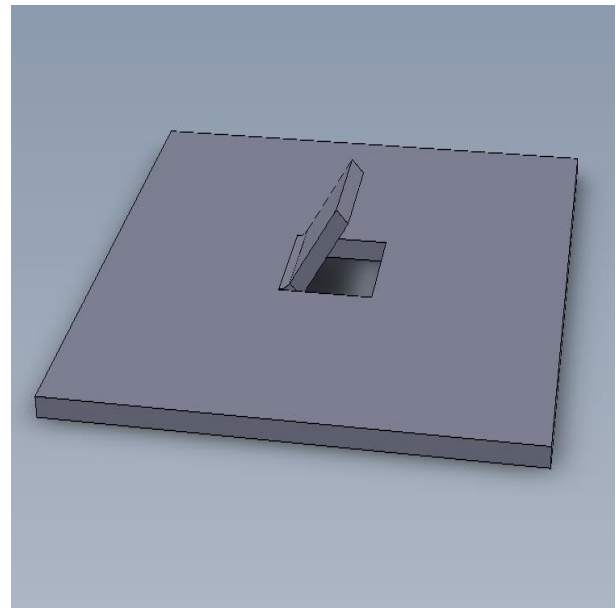


Fig. 8 Model of a lifted orifice

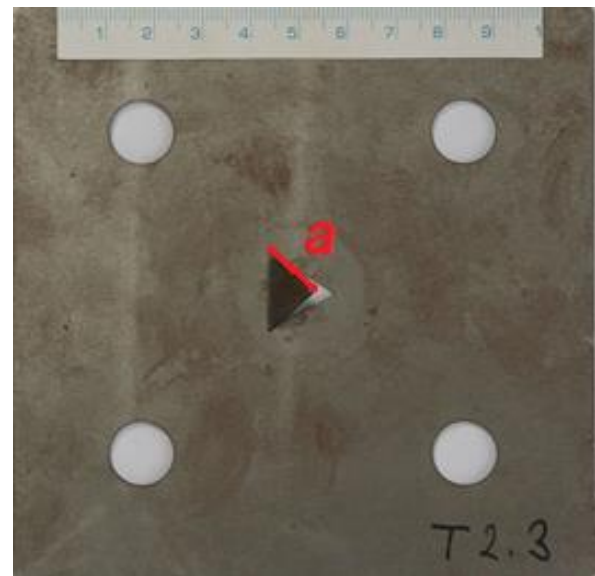


Fig. 9 Example of the screen with irregular orifice shape – lifted triangle. a= 14.1 mm

The calculation of the discharge coefficient:

Discharge coefficient we get by calculations from experimental data, which we get from measurement outputs in the form of:

- V vessel volume [m³]
- P_{am} atmospheric pressure [Pa]
- τ_i time of i -th measured point [s]
- P_i gas pressure in the vessel at the time τ_i [Pa]
- T_i gas temperature in the vessel at the time τ_i . [K]
- M molar mass of the gas [kg mol⁻¹]

Following from measured data we can evaluate for each time τ_i the mass of the gas (retention) m_i in the vessel, using state equation of ideal gas [9]:

$$m_i = \frac{P_i VM}{RT_i} \quad (2.1)$$

where R is the universal gas constant, $R=8.314 \text{ J K}^{-1} \text{ mol}^{-1}$.

From the time course of gas retention we can get the mass flow of leaking gas.

We will further modify the equation 1 by setting the discharge coefficient to one, and effectively leaving it out of the equation. Resulting mass flow will be theoretical maximum flow which would exist if there were no contraction and losses in the orifice.

$$\dot{m}_{theor} = S\rho v \quad (2.2)$$

To evaluate theoretical flow, we need independent way to calculate the gas velocity v in the orifice.

Let's define critical pressure ratio β [10]

$$\beta = \frac{P_{atm}}{P_{crit}} = \left(\frac{2}{\kappa + 1} \right)^{\frac{\kappa}{\kappa + 1}} \quad (2.3)$$

where P_{crit} is critical pressure, P_{atm} is atmospheric pressure and κ is isentropic coefficient.

While the pressure is in critical area ($P_{atm}/P_i < \beta$) we replace gas velocity v with the formula:

$$v_{crit} = \sqrt{2 \frac{\kappa RT_i}{(\kappa + 1)M}} \quad (2.4)$$

For the pressure in sub-critical area ($P_{atm}/P_i > \beta$) we get for the gas velocity [10]:

$$v_{subcrit} = \sqrt{2 \frac{RT_i}{KM} \left[1 - \left(\frac{P_{atm}}{P_i} \right)^\kappa \right]} \quad (2.5)$$

where K is a constant which depends on isentropic coefficient κ :

$$K = \frac{\kappa - 1}{\kappa} \quad (2.6)$$

The mass of the gas can be calculated from the state equation of the ideal gas. Following variables are put into equation 2.2:

- v gas velocity v_{crit} (2.4) or $v_{subcrit}$ (2.5) [$\text{m}\cdot\text{s}^{-1}$]
- S cross-section orifice flow area [m^2]
- V gas retention in vessel [m^3]
- m mass of the gas retention in vessel [kg]
- \dot{m} mass flow rate of gas [kg s^{-1}]

Actual experimentally observed values of the gas mass flow \dot{m}_{exp} are obtained by numeric derivation $dm/d\tau$ of the measured course of decreasing gas retention during the experiment.

Finally, the discharge coefficient α is calculated as a ratio of experimental mass flow to theoretical adiabatic mass flow

$$\alpha = \frac{\dot{m}_{exp}}{\dot{m}_{theor}} \quad (2.7)$$

3. Results

All the measurements are carried out for methane.

Results of the experiments are visualized in form of graphs of dimensionless discharge coefficient dependency on dimensionless ratio P_{atm}/P . Dotted vertical line indicates critical pressure ratio $P_{atm}/P = 0,5429$.

Thin orifices in circular shape have been tested such way and results are shown in the Fig. 10 for the smallest to largest diameters accordingly. For orifices of larger diameter the discharge coefficient decreases faster with decreasing pressure than for smaller diameters. The discharge coefficient is more stable for bigger diameters.

Furthermore, thick circular shape orifices have been tested (2.x - the table 1) and rectangular (Cx.x - the table 1), triangular (Tx.x - the table 1) and slot shapes (Sx - the table 1) as well.

Thick circular screens have more stable discharge coefficient comparing to thin circular screens. For bigger diameters discharge coefficient decreases rapidly for low pressure similar to thin circular orifices (Fig. 11).

The highest discharge coefficient from the tested triangular orifices has screen T1.1, which area is a bit smaller than the circular screen 1.4. Screen T2.1 is full shape triangle screen which area corresponds to circular screen 1.6. The screens T2.2 and T2.3 have the lifted flap, which is also evident in the Fig. 9. The flap in the screen T2.2 is lifted under lower angle (the flap is more restricted) than flap T2.3 and also the discharge coefficient for flap T2.3 is higher than the flap over the screens in case of flap T2.2. So-called *downstream* mark describes the direction of the flap into a vessel, therefore against the gas flow direction. So-called *upstream* mark describes the direction in the gas flow. The discharge coefficient is higher for lifted flap *upstream* than for lifted flap *downstream* evidently (see Fig. 13).

In case of the square orifice have the orifices with full flow nearly the same value of discharge coefficients. The discharge coefficient is higher for lifted flap *upstream* than for lifted flap *downstream* evidently so as at the triangular orifice (see Fig. 12).

From all the types of orifices has the biggest discharge coefficient a rectangular narrow slot. In case of rectangular slots, if the slot is narrower, the discharge coefficient is higher (see Fig. 14).

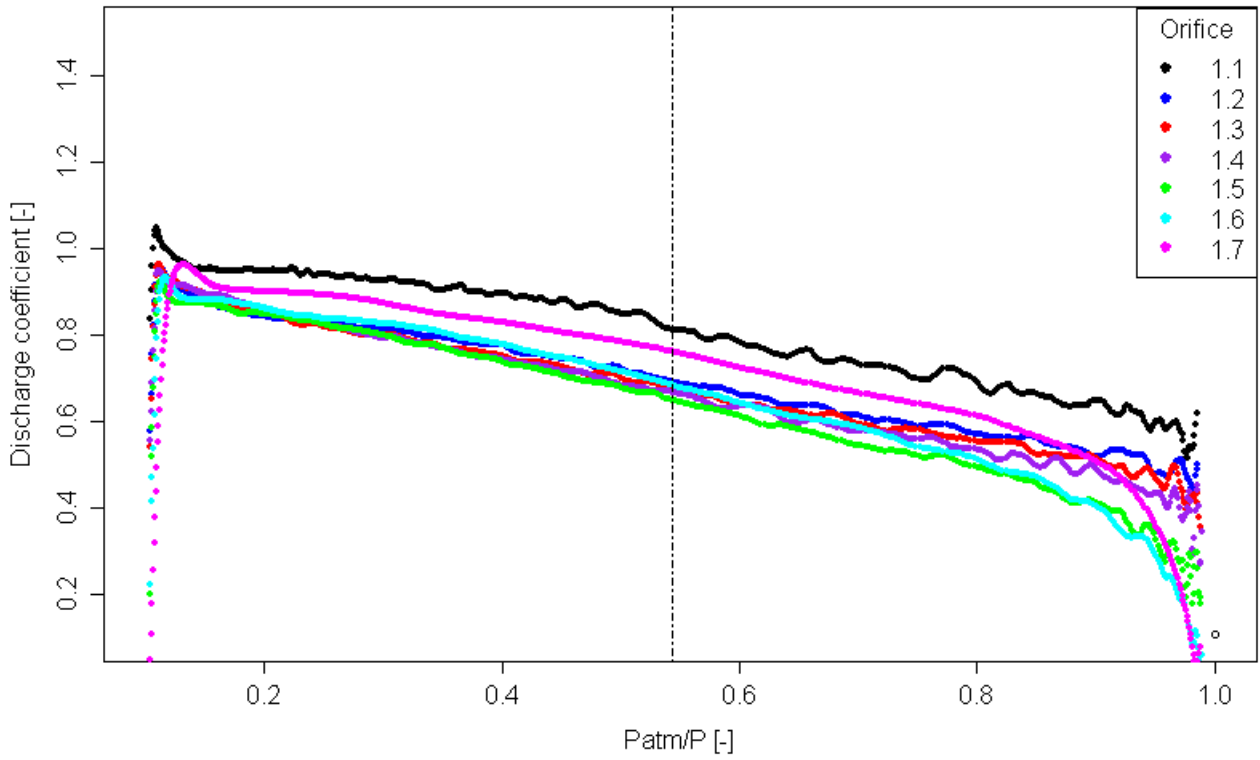


Fig. 10 Dependency of discharge coefficient on p_{atm}/p for thin circular orifices

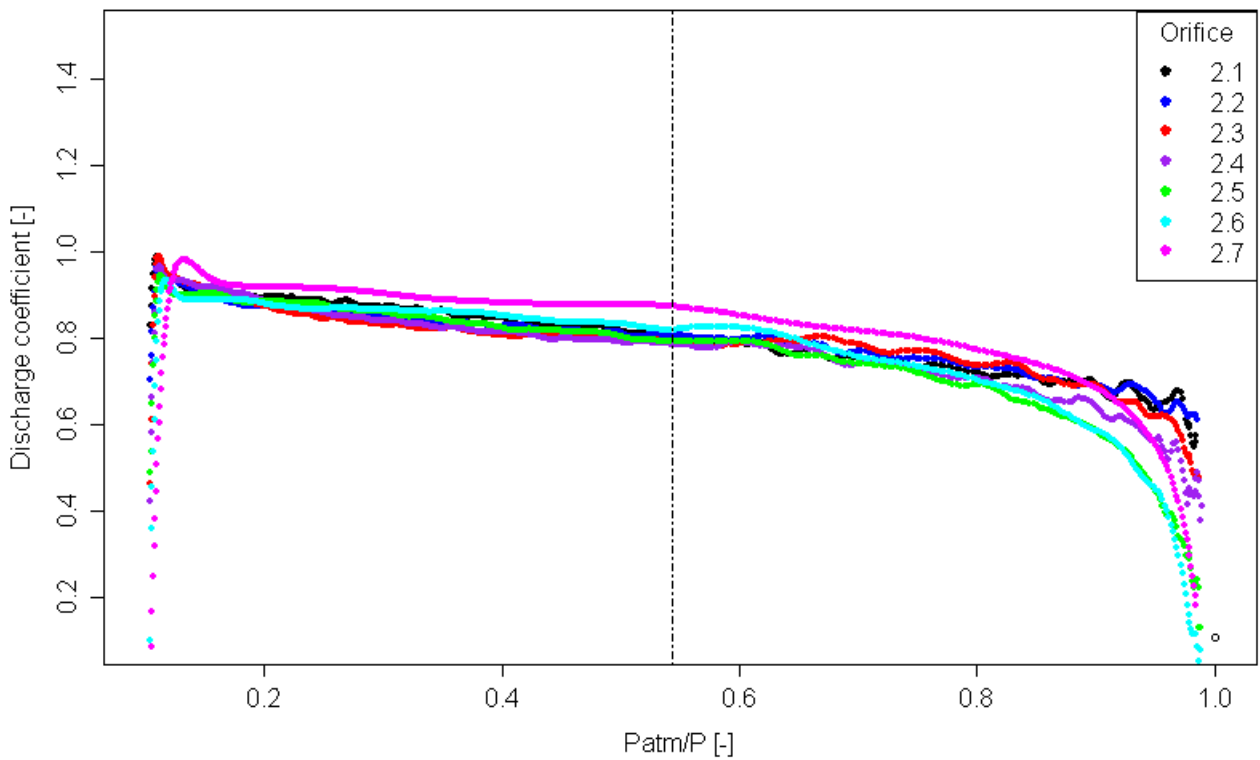


Fig. 11 Dependency of discharge coefficient on p_{atm}/p for thick circular orifices

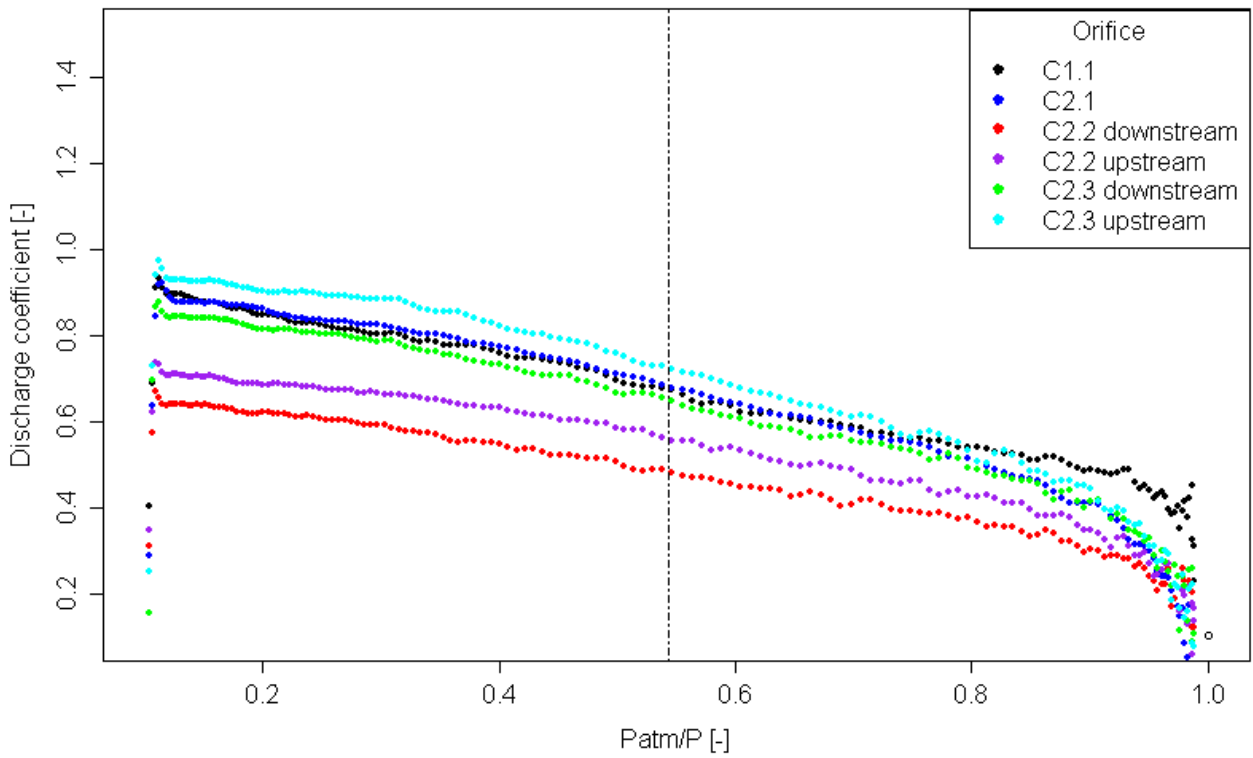


Fig. 12 Dependency of discharge coefficient on p_{atm}/p for square orifices

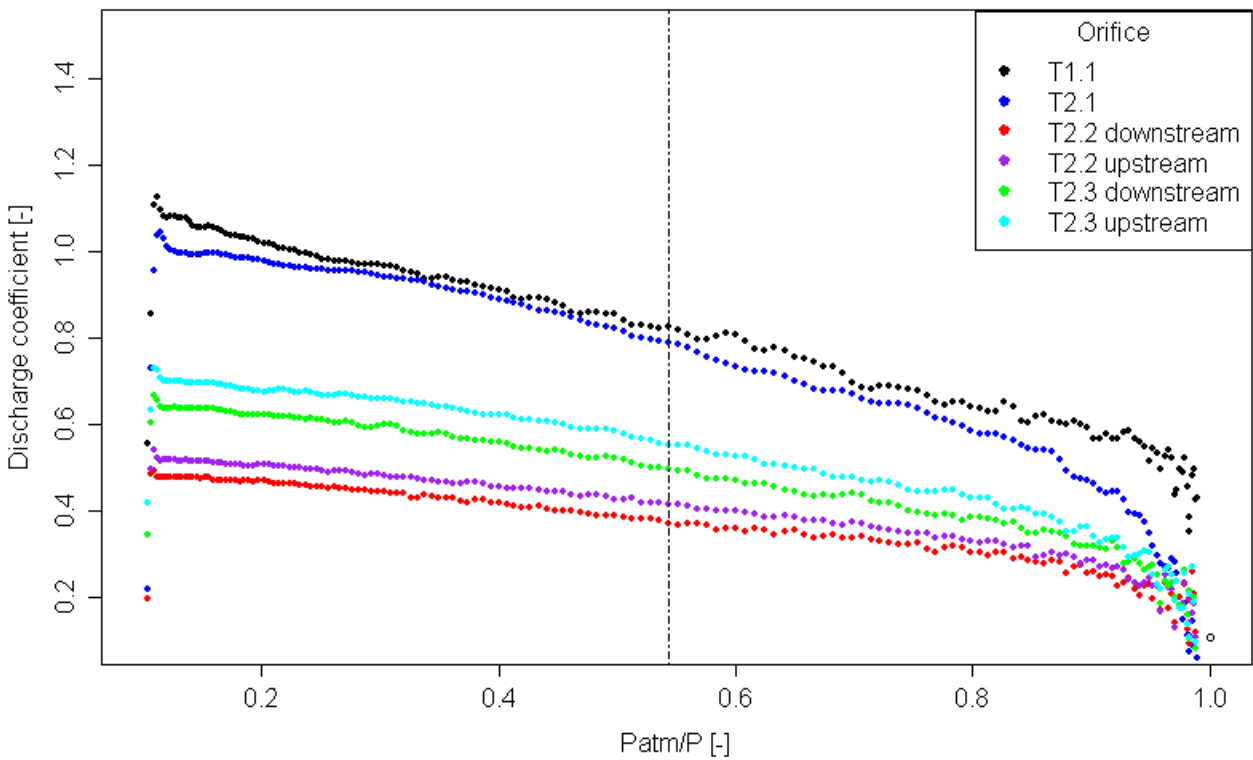


Fig. 13 Dependency of discharge coefficient on p_{atm}/p for triangular orifices

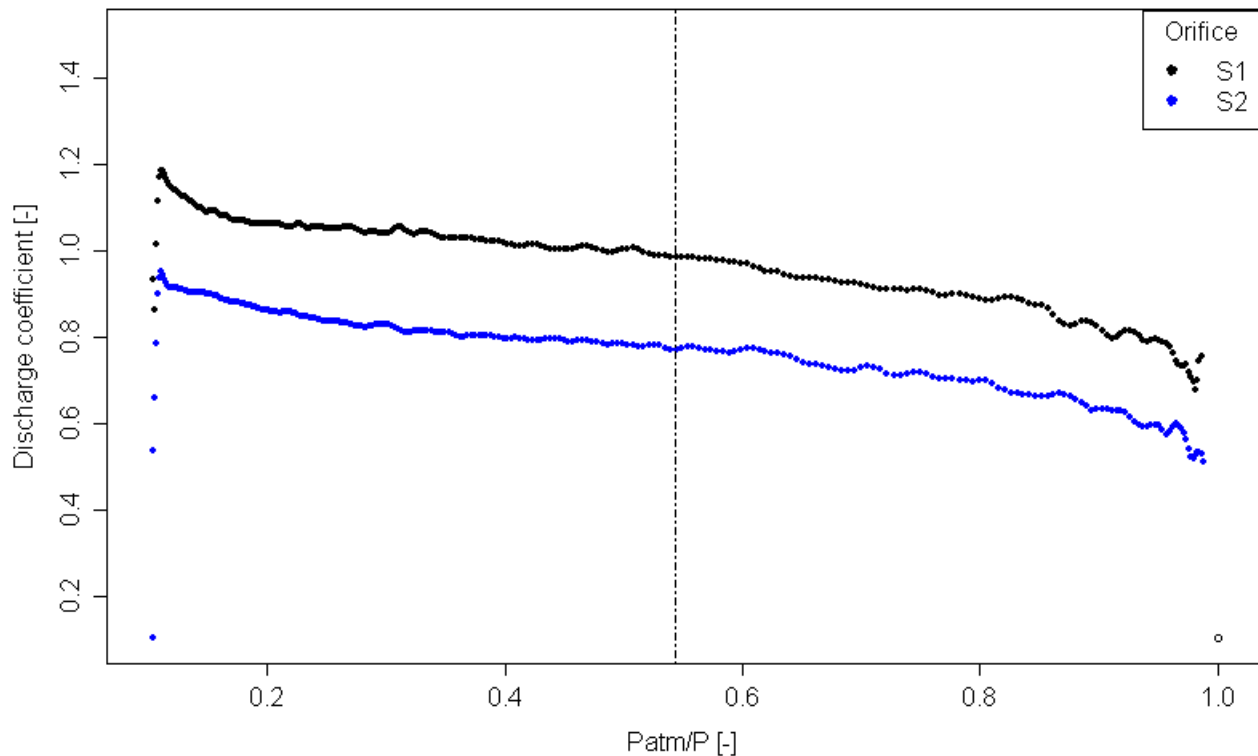


Fig. 14 Dependency of discharge coefficient on p_{atm}/p for slot orifices

4. Conclusion

It is possible to determine discharge coefficients for various orifices with this apparatus. Orifices of regular and irregular shape were created to simulate different pipeline disruptions. Dimensions of the orifices are limited by valve size, which is 25 mm. Overpressure in the vessel can be freely set up to 1 MPa. It is also possible to use the apparatus for measuring various types of inert gases and methane.

Literature

1. Lapple, C. E. Isothermal and Adiabatic Flow of Compressible Fluids. *AIChE*. 1943, 39, s. 385–428
2. Bragg, S. L. Effect of Compressibility on the Discharge Coefficient of Orifices and Convergent Nozzles. *Journal of Mechanical Engineering Science*. 1960, 2, 1, s. 35–44.
3. Benson, R. S. – Pool, D. The Compressible Flow Discharge Coefficients for a Two-Dimensional Slit. *International Journal of Mechanical Sciences*. 1965b, 7, s. 337–353
4. Deckker, B. E. L. Compressible Flow through Square Edge Rectangular Orifices. *Proceedings of the Institution of Mechanical Engineers*. 1978, 192, 1, s. 277–288.
5. Deckker, B. E. L. – Chang, Y. F. Paper 19: Slow Transient Compressible Flow through Orifices. *Proceedings of the Institution of Mechanical Engineers, Conference Proceedings*. 1967, 182, 8, s. 175–183.
6. Chang, Y. F. Transient Effects in the Discharge of Compressed Air from a Cylinder through an Orifice. PhD. Thesis, University of Saskatchewan, 1968
7. Johnston, S. C. A Characterization of Unsteady Gas Discharge from a Vessel, Dissertation, University of California, Davis, 1974
8. Noskevič J. a kol., *Mechanika tekutin*, SNTL/ALFA, Praha, 267-272 (1987)
9. Novák J.: *Termodynamické vlastnosti plynů*. Praha : VŠCHT, 2007 Nožička, J., *Dynamika plynů*, Vydavatelství ČVUT, Praha 2005, 155 stran, ISBN 80-01-03300-7
10. Team of authors, *Methods for the calculation of physical Effects CPR 14E*, second edition, Committee for Prevention of Disaster, TNO, (1991).